Pergamon

Int. J. Solids Structures Vol. 35, No. 11, pp. 963–979, 1998

0020–7683/98 $19.00 + .00

PII: S0020–7683(96)00231–4

DYNAMIC RESPONSE OF FULLY-CLAMPED LAMINATED COMPOSITE PLATES SUBJECTED TO LOW-VELOCITY IMPACT OF A MASS

LU CHUN and K. Y. LAM
Department of Mechanical and Production Engineering, National University of Singapore, 10 Kent Ridge Crescent, Singapore 0511

(*Received* 15 *July* 1994; *in revised form* 18 *October* 1996)

Abstract—A numerical method for the calculation of dynamic response of laminated composite plates under low-velocity impact is proposed. The non-linear, second-order differential governing equations are derived by the Lagrange's principle and the Hertzian contact law. The governing equations are decoupled according to the second-order terms by the method of principal transformation, and then solved numerically. The dynamic response of fully clamped cross and angle ply laminated plates struck by a mass is investigated. The contact force, deformation, energy transferred and stresses in the composite plates are presented. Good agreement is achieved when compared with results available in the literature. © 1998 Elsevier Science Ltd.

INTRODUCTION

The impact problem has received wide attention for many years. Dynamic response of structures under impact loading is an important factor needed to be considered in design. The basic approach in this area was proposed by Timoshenko (1913). He combined the Euler beam theory and the Hertzian contact law to study the low-velocity impact problem between a steel ball and an elastic beam. The approach was further extended to the analysis of isotropic plates and shells subjected to impact loading. Simplified models of the impact problem were also introduced by various authors (Lee, 1940; Greszczuk, 1982; Lee *et al.*, 1983; Shivakumar *et al.*, 1985) to overcome the difficulty in solving the non-linear integral equation caused by the non-linear relationship in the Hertzian contact law. When the dynamic response of the composite structures under an impact loading is investigated, the special properties of composite materials must be considered.

Composite materials have been widely utilised in many industries, due to their high strength and stiffness to weight ratios. The applications of laminated composite plates and shells for aerospace and aircraft structures when subjected to impact have become a significant topic in the past two decades. Sun and Chattopadhyay (1975), Dobyns (1981), and Ramkumar and Chen (1983) employed the first-order shear deformation theory developed by Whitney and Pagano (1970), and used in conjunction with the classical Hertzian contact law or an assumed known contact force to study the impact of laminated composite plates. The three-dimensional finite element method (Lee *et al.*, 1984; Sun and Chen, 1985; Wu and Chang, 1989; Sun and Liou, 1989) and spline approximation method (Bogdanovich and Iarve, 1992) are also used to perform the dynamic analysis of laminated plates under impact loading. Shivakumar *et al.* (1985) proposed a simple model to predict the impact force and duration on circular laminated composite plates. In their method, the composite plate was modelled to a three-spring system and the stiffness of the springs must be known first. Tan and Sun (1985), Lin and Lee (1990) examined the impact problem of the laminated plates and shells by the statical indentation law presented by Tan and Sun (1985), instead of using the classical Hertzian contact law. The non-Hertzian contact impact was considered by Keer *et al.* (1986, 1987), the method of combining the overall deformation of the structure and local deformation in the contact area was used to predict the impact response of transversely isotropic beams and plates.

In general, it is impossible to obtain the exact solution for impact problem, except by ignoring the local contact deformation or pre-assuming the contact force. From the calculations in the present paper, it can easily be seen that the energy absorbed by the local deformation is considerable during impact and the phenomena of the contact force with the multiple peak values are observed in all the three types of laminations with various stacking sequences. The accuracy of results obtained from the simplified methods hence cannot be assured. In the works available from the literature, in which the non-linearity of impact problem was considered, the emphasis was usually on the derivation of the non-linear integral equation of motion for the contact force; the equation was then solved by the small-time increment method. From the numerical point of view, solving a non-linear integral equation which includes the summation of function series is much more difficult than solving the equivalent non-linear differential equations.

In this paper, the response of laminated composite plates under the low-velocity impact is analysed. The contact area between the striker and plate is very small, assuming to be a point. The Hertzian contact law is then employed to evaluate the contact force. Unlike most of other previous works involving the derivation of the non-linear integral equation for the contact force, the displacement of the striker and generalised displacements of the composite plate are taken to be the generalised co-ordinates of the system, which consists of the striker and plate. Based on the higher order shear theory given by Reddy (1984), the non-linear differential equations of motion are then derived by using the Lagrangian principle and Hertzian contact law with the modified contact constant. The governing equations are decoupled to the second-order terms by using the transformation of principal and then solved numerically. The contact force, deformation, stresses and energy transferred from the striker to the composite plates are presented. The comparison of the present numerical results with the works in the open literature shows good agreements.

GOVERNING EQUATIONS

Consider the system that includes a laminated composite plate and striker. The origin of the Cartesian co-ordinate system is located in the middle plane of the laminated plate, and the z-axis is perpendicular to the mid-plane as shown in Fig. 1. The dimensions of the laminated plate along the x and y directions are a and b, respectively. The laminated plate is composed of K orthotropic layers, and the total thickness is h. According to Reddy's higher-order theory (1984), the displacement field is expressed as

$$u = z\left(\psi_x - \frac{4}{3}\left(\frac{z}{h}\right)^2\left(\psi_x + \frac{\partial w}{\partial x}\right)\right)$$

$$v = z\left(\psi_y - \frac{4}{3}\left(\frac{z}{h}\right)^2\left(\psi_y + \frac{\partial w}{\partial y}\right)\right)$$

$$w = w(x, y, t) \tag{1}$$

where ψ_x, ψ_y are the mid-plane slopes in the x–z and y–z planes, respectively. In eqn (1),

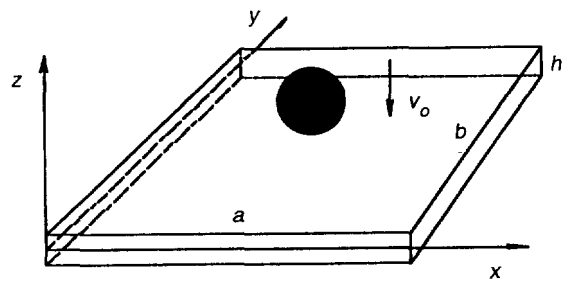

Fig. 1. System configuration.

the in-plane displacements are assumed to be negligible when compared with the flexural displacements.

The strain distributions throughout the laminated plate are given by

$$\varepsilon_x = \frac{\partial u}{\partial x}, \quad \varepsilon_y = \frac{\partial v}{\partial y}, \quad \varepsilon_{xy} = \frac{\partial u}{\partial y} + \frac{\partial v}{\partial x}$$

$$\varepsilon_{yz} = \frac{\partial v}{\partial z} + \frac{\partial w}{\partial y}, \quad \varepsilon_{xz} = \frac{\partial u}{\partial z} + \frac{\partial w}{\partial x}. \tag{2}$$

For an orthotropic layer, the constitutive relationship referred to the natural axes of the layer can be written as

$$\begin{bmatrix} \bar{\sigma}_x \\ \bar{\sigma}_y \\ \bar{\sigma}_{xy} \end{bmatrix} = \begin{bmatrix} \bar{Q}_{11} & \bar{Q}_{12} & 0 \\ \bar{Q}_{12} & \bar{Q}_{22} & 0 \\ 0 & 0 & \bar{Q}_{66} \end{bmatrix} \begin{bmatrix} \bar{\varepsilon}_x \\ \bar{\varepsilon}_y \\ \bar{\varepsilon}_{xy} \end{bmatrix} \tag{3a}$$

$$\begin{bmatrix} \bar{\sigma}_{yz} \\ \bar{\sigma}_{xz} \end{bmatrix} = \begin{bmatrix} \bar{Q}_{44} & 0 \\ 0 & \bar{Q}_{55} \end{bmatrix} \begin{bmatrix} \bar{\varepsilon}_{yz} \\ \bar{\varepsilon}_{xz} \end{bmatrix} \tag{3b}$$

where the top bar represents the quantities in the natural co-ordinate system. Q_{ij} are the material parameters.

In the plate co-ordinates, the relationship is transformed to

$$\begin{bmatrix} \sigma_x \\ \sigma_y \\ \sigma_{xy} \end{bmatrix} = \begin{bmatrix} Q_{11} & Q_{12} & Q_{16} \\ Q_{12} & Q_{22} & Q_{26} \\ Q_{16} & Q_{26} & Q_{66} \end{bmatrix} \begin{bmatrix} \varepsilon_x \\ \varepsilon_y \\ \varepsilon_{xy} \end{bmatrix} \tag{4a}$$

$$\begin{bmatrix} \sigma_{yz} \\ \sigma_{xz} \end{bmatrix} = \begin{bmatrix} Q_{44} & Q_{45} \\ Q_{45} & Q_{55} \end{bmatrix} \begin{bmatrix} \varepsilon_{yz} \\ \varepsilon_{xz} \end{bmatrix} \tag{4b}$$

where Q_{ij} are the transformed material constants.

In the present study the vibration of the striker caused by the impact is ignored, and hence the kinetic and potential energies of the system can be represented in terms of the displacements of the laminated plate and striker. Let m_s, W_s denote the mass and displacement of the striker; the total kinetic energy of the system is given by

$$T = \frac{1}{2} \sum_{k=1}^{K} \int_{V_k} \rho_k [\dot{U}]^T [\dot{U}] \cdot \mathrm{d}V + \frac{1}{2} m_s \dot{W}_s^2 \tag{5}$$

where $[U] = [u \quad v \quad w]^T$ and the top denotes the derivative with respect to time; ρ_k is the density of the k-th layer.

The unknown contact force f_c can be treated as an internal force of the system. Upon the impact, the relationship between the contact force f_c and the indentation of the plate, $w(x_s, y_s, t) - W_s(t)$ is given by the Hertzian contact law (Hertz, 1881) as

$$f_c = k_c (w(x_s, y_s, t) - W_s)^{1.5} \tag{6}$$

where k_c is the modified constant (Yang and Sun, 1982) for the composite material, and (x_s, y_s) denotes the impact point on the top surface of the laminated plate.

Once the contact force f_c is expressed by the displacements, the potential energy of the system can be written as

$$P = \frac{1}{2}\sum_{k=1}^{K}\int_{V_k}[\sigma]^T\cdot[\varepsilon]\,\mathrm{d}V + \frac{2}{5}k_c(w(x_s,y_s,t)-W_s)^{5/2}. \tag{7}$$

The displacements of the laminated plate are assumed to be able to separate into the functions of time and position. Then, the mid-plane slopes and transverse displacement can be written

$$\begin{bmatrix}\Psi_x\\ \Psi_y\\ w\end{bmatrix} = \begin{bmatrix}[\varphi_{xi}(x,y)] & 0 & 0\\ 0 & [\varphi_{yi}(x,y)] & 0\\ 0 & 0 & [\varphi_{zi}(x,y)]\end{bmatrix}\begin{bmatrix}[A_i(t)]\\ [B_i(t)]\\ [C_i(t)]\end{bmatrix} \quad i=1,2,\ldots,n \tag{8}$$

where $[A_i]$, $[B_i]$ and $[C_i]$ are the $3n$ coefficients to be determined, and $[\varphi_{xi}]$, $[\varphi_{yi}]$ and $[\varphi_{zi}]$ consist of the complete function series of the position, which must satisfy the boundary conditions of the impacted plate.

Substituting eqn (8) into the expressions of the displacements, velocity, strains and stresses, the kinetic and potential energies of the system can therefore be expressed in terms of the generalised co-ordinates of $[A_i]$, $[B_i]$, $[C_i]$ and W_s of the system.

In order to obtain the governing equations of the system, the Lagrange's equations are applied to the kinetic and potential energies

$$\frac{\mathrm{d}}{\mathrm{d}t}\left(\frac{\partial T}{\partial \dot{p}_j}\right) - \frac{\partial T}{\partial p_j} + \frac{\partial P}{\partial p_j} = 0 \quad j=1,2,\ldots,3n+1 \tag{9}$$

where $[p] = [[A_i] \quad [B_i] \quad [C_i] \quad W_s]$. By substituting T and P into eqn (9), and collecting the coefficients of the generalised co-ordinates of $[A_i]$, $[B_i]$, $[C_i]$, W_s and the non-linear term, the following non-linear second-order partial differential equations are obtained,

$$\begin{bmatrix}[M] & [0]_d\\ [0]_d^T & m_s\end{bmatrix}\cdot\begin{bmatrix}[\ddot{A}_i]\\ [\ddot{B}_i]\\ [\ddot{C}_i]\\ \ddot{W}_s\end{bmatrix} + \begin{bmatrix}[K] & [k']\\ [0]_d^T & -k_c\end{bmatrix}\cdot\begin{bmatrix}[A_i]\\ [B_i]\\ [C_i]\\ \left(\sum_{i=1}^{n} C_i\varphi_{zi}(x_s,y_s) - W_s\right)^{3/2}\end{bmatrix} = 0 \tag{10}$$

where

$$[k'] = [[0]_k \quad [0]_k \quad [k_c\cdot\varphi_{zi}(x_s,y_s)]]^T \tag{11}$$

and $[M]$ and $[K]$, which are given in the Appendix, are the $3n\times 3n$ mass and stiffness matrices of the laminated plate with fully clamped boundary conditions, and the dimensions of $[0]_d$ and $[0]_k$ are $3n\times 1$ and $n\times 1$, respectively.

It is assumed that the laminated plate is initially at rest, so that the initial conditions of the system can be expressed as

$$[U] = [\dot{U}] = 0; \quad W_s = \frac{h}{2}, \quad \dot{W}_s = V_0 \tag{12}$$

where V_0 is the initial impact velocity.

It is impossible to obtain a set of analytical solutions to the non-linear governing eqns (12), and hence numerical techniques are applied in this work.

SOLUTION PROCEDURE

In order to use numerical techniques to solve the governing equations derived in the last section, the second derivative terms in the equations must be decoupled. The governing equations can be rewritten in the following form

$$[M]\cdot\begin{bmatrix}[\ddot{A}_i]\\ [\ddot{B}_i]\\ [\ddot{C}_i]\end{bmatrix}+[K]\cdot\begin{bmatrix}[A_i]\\ [B_i]\\ [C_i]\end{bmatrix}=-\begin{bmatrix}[0]_k\\ [0]_k\\ [\varphi_{zi}(x_s,y_s)]\end{bmatrix}k_c\left(\sum_{i=1}^{n}C_i\varphi_{zi}(x_s,y_s)-W_s\right)^{3/2}$$

$$m_s\ddot{W}_s=k_c\left(\sum_{i=1}^{n}C_i\varphi_{zi}(x_s,y_s)-W_s\right)^{3/2}. \tag{13}$$

Let ω_i represent the frequency of the free vibration of the laminated plate with fully fixed boundary conditions, and $[V]$ denotes the normalised mode shape matrix. Then the following principal co-ordinate transformation is adopted,

$$\begin{bmatrix}[A_i(t)]\\ [B_i(t)]\\ [C_i(t)]\end{bmatrix}=\begin{bmatrix}[V_1]\\ [V_2]\\ [V_3]\end{bmatrix}\cdot[q_j(t)]\quad j=1,2,\ldots,3n \tag{14}$$

where $q_j(t)$ is called the principal co-ordinate of the plate and $[V]=[[V_1]\quad[V_2]\quad[V_3]]^T$.

The orthogonality of the normal modes can be expressed as

$$[V]^T[M][V]=[I]$$
$$[V]^T[K][V]=[\omega_i^2] \tag{15}$$

where $[\omega_i^2]$ is the diagonal matrix which consists of the $3n$ frequencies of the laminated plate and $[I]$ is the identity matrix.

Because the coefficients C_i appear in the non-linear terms of the governing equations, C_i must be written in terms of the principal co-ordinates as follows:

$$C_i=\sum_{j=1}^{3n}V_3^{ij}q_j. \tag{16}$$

By substituting eqns (14) and (16) into eqn (13), and premultiplying $[V]^T$, we can then obtain the governing equations of the system in terms of the principal co-ordinates of the plate and displacement of the striker. The second-order terms in the equations are hence decoupled into

$$[\ddot{q}_i]=-[V]^T\cdot\begin{bmatrix}[0]_k\\ [0]_k\\ [\varphi_{zi}(x_s,y_s)]\end{bmatrix}\cdot k_c\left(\sum_{i,j}V_3^{ij}\varphi_{zi}(x_s,y_s)q_j-W_s\right)^{3/2}-[\omega_i^2q_i]$$

$$\ddot{W}_s=\frac{k_c}{m_s}\left(\sum_{i,j}V_3^{ij}\varphi_{zi}(x_s,y_s)q_j-W_s\right)^{3/2} \tag{17}$$

where $[q_i]=[q_1\quad q_2\quad\ldots\quad q_{3n}]^T$ and $[\omega_i^2q_i]=[\omega_1^2q_1\quad\omega_2^2q_2\quad\ldots\quad\omega_{3n}^2q_{3n}]^T$.

When the time is set to zero, the initial conditions can be derived for the principal co-ordinates of the plate from eqns (8), (12) and (14) as follows,

$$q_j = \dot{q}_j = 0 \quad j = 1, 2, \ldots, 3n. \tag{18}$$

Equations (17) and (18) can then be numerically solved by means of the Runge–Kutta–Nystrom techniques (NAG, 1991). From the governing equations, the contact force, displacement of the striker and deflection of the laminated plate may be calculated. The strains and stresses in the plate can then be obtained from the eqns (2) and (3).

NUMERICAL RESULTS AND DISCUSSIONS

1. *Isotropic plate under impact*

For verification of the capability and applicability of the proposed method, a classical impact problem of plate (Karas, 1939) is calculated and compared with previously published works.

A square steel plate having the simply supported boundary conditions at four edges is impacted by a steel ball. The impact point is on the centre of the plate. Karas calculated the problem by the small-time increment method, while Wu and Chang (1989) solved it by finite element method. The contact force, deflections and velocity were provided in their publications. The details of the geometrical configuration and material properties are given as follows:

$$E = 206\,\text{GPa}, \quad G = 79.85\,\text{GPa}, \quad \nu = 0.28, \quad \rho = 7.833 \times 10^3\,\text{kg/m}^3,$$

$$a = b = 0.2\,\text{m}, \quad h = 8 \times 10^{-3}\,\text{m}, \quad R = 0.01\,\text{m}, \quad V_0 = -1\,\text{m/s}, \quad m_s = 0.0328\,\text{kg}$$

where E, G are Young's and shear moduli of steel, ν and ρ are steel's Poisson ratio and density, respectively. a and b are dimensions of the plate along x and y axes, h is the thickness of the plate; R and V_0 are the radius and initial velocity of the steel striker.

The simple polynomial series, which satisfy the simply supported boundary condition

$$w = 0 \quad \text{at the lines} \begin{cases} x = 0, a \\ y = 0, b \end{cases} \tag{19}$$

are selected to compose φ_{xi}, φ_{yi} and φ_{zi}. In the calculations, the first 49 terms of the polynomial series are taken.

Results obtained by using the present formulations are compared with two solutions reconstructed from the published papers and are plotted in Figs 2–4. The Imperial units

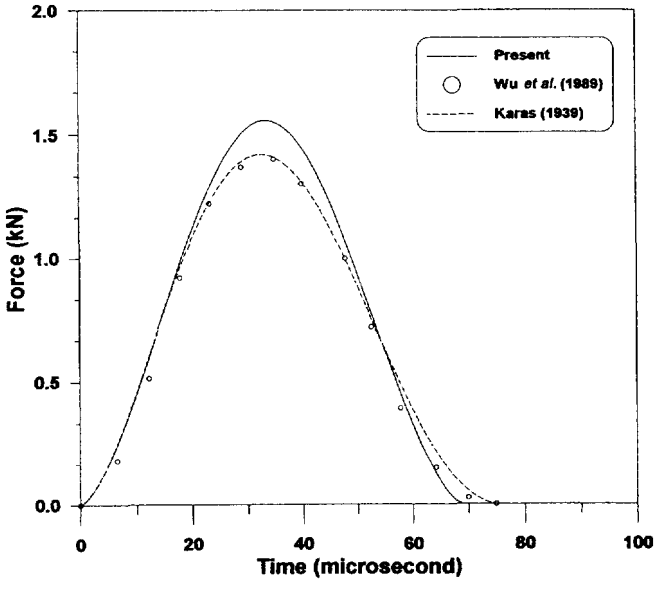

Fig. 2. Comparison of the contact forces.

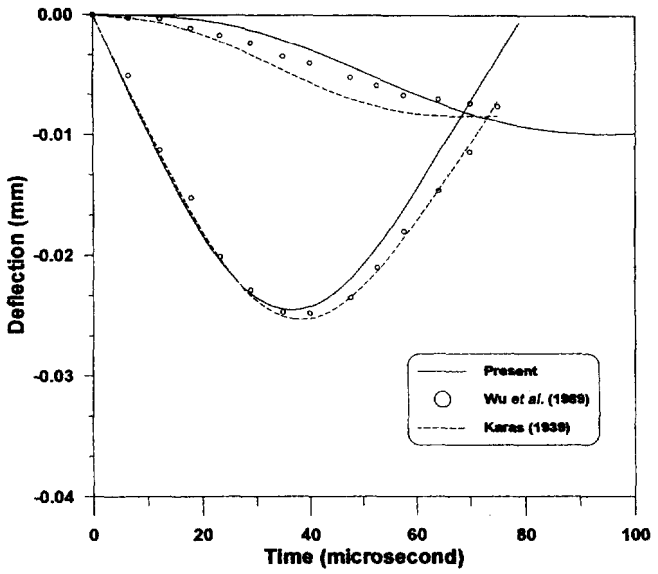

Fig. 3. Comparison of the displacements of the striker and plate at the contact point.

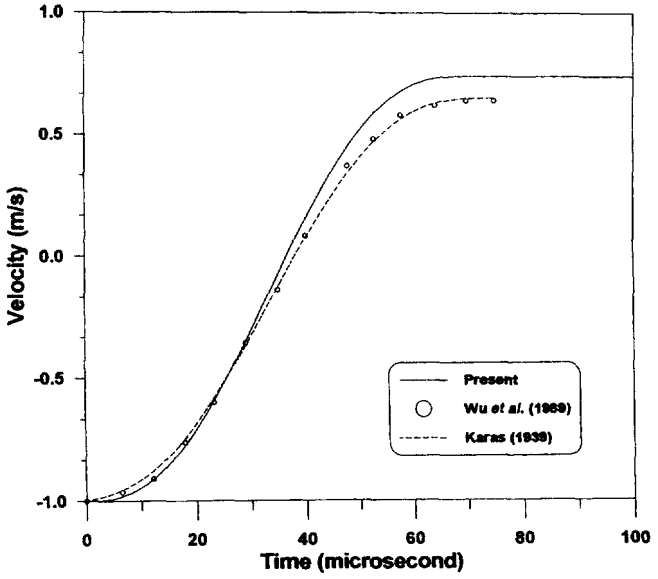

Fig. 4. Comparison of striker's velocity.

used in the papers (Wu and Chang, 1989) are changed to SI system. The dash lines represent Karas' work and open circles are finite element results by Wu and Chang. The time histories of the contact force and displacements of the striker and plate at the impact point are given in Figs 2 and 3. The history of the velocity of the striker is plotted in Fig. 4. From the figures, it can be seen that very good agreement is achieved. The energy transformation between the striker and plate is also obtained by the proposed method and plotted in Fig. 5; it can be found that the energy absorbed by the local deformation is considerable during impact.

2. *Laminated plates under impact*

By using the present method, the numerical results can be obtained for laminated composite plates with arbitrary stacking sequence and boundary conditions subjected to a transverse impact. Due to the lack of the impact response for clamped composite plate in the literature, the solutions of fully clamped cross and angle ply laminated plates under central impact are presented here.

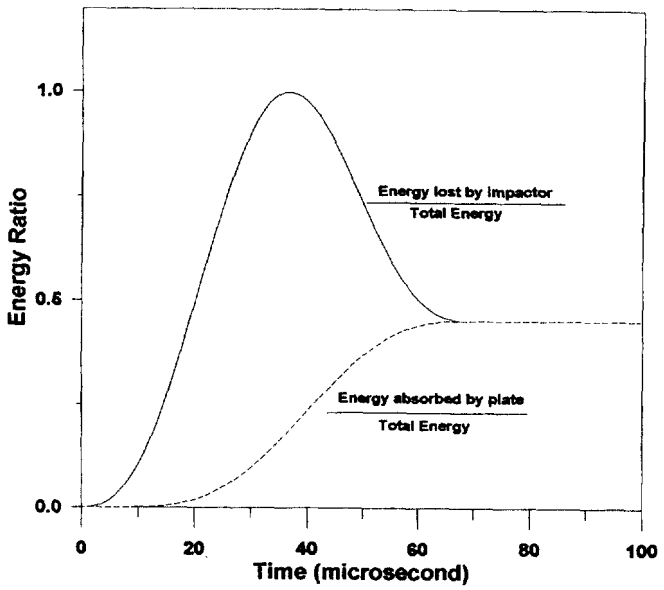

Fig. 5. Energy changes of the striker and plate during impact.

For the fully clamped laminated plate, the function series φ_{xi}, φ_{yi} and φ_{zi} are selected to satisfy the fixed boundary conditions

$$\Psi_x = \Psi_y = w = \frac{\partial w}{\partial x} = \frac{\partial w}{\partial y} = 0 \quad \text{at the lines} \begin{cases} x = 0, a \\ y = 0, b \end{cases}. \tag{20}$$

The composite plates under investigation are made by graphite-epoxy AS-3501-6 and fully fixed on edges. Three types of laminations, three layers cross-ply (0/90/0) and angle-ply (30/−30/30), (−30/0/30), are used in analysis. Each lamina has the same thickness and material properties. The effects of ply orientation on the contact force, displacement and stress distributions are presented.

The laminated plates are impacted by a striker with velocity $V_0 = -22.6$ m/s. The mass of the striker is $m_s = 0.014175$ kg. The modified contact constant k_c is 1×10^8 N/m$^{1.5}$. The impact point is on the centre of the lamination. The geometrical and material properties of the composite plate are given as follows

$$E_1 = 142.73\,\text{GPa}, \quad E_2 = 13.79\,\text{GPa}, \quad G_{12} = 4.64\,\text{GPa}, \quad \nu_{12} = 0.3,$$
$$\rho = 1.61 \times 10^3\,\text{kg/m}^3, \quad a = b = 0.14\,\text{m}, \quad h = 3.81 \times 10^{-3}\,\text{m}.$$

The contact forces are given in Fig. 6 as function of time. It is worth noting that the contact forces have more than one peak value during the impact. The contact forces reach the first peak points around 100 ms after the contact happened for all the three laminations. Then, the contact forces decrease rapidly. At 250 ms and 440 ms, the contact force on the cross-ply laminated plate runs to its second and third peak values, which are much smaller than the first one. For the angle-ply laminations, the contact forces almost drop down to zero from 200 to 300 ms, during which the striker and plates only keep loose contact. Then, the contact forces start to increase to the second peak values around 400 ms. The contact force with multiple peaks was also found by Schonberg *et al.* (1987).

The time histories of the striker velocities are presented in Fig. 7. At 140 ms, the values of velocities decline to zero, which occurs after 40 ms when the contact forces reach the maximum values. This is caused by the local deformation in the laminated plates. When the striker is separated with the composite plates, the velocities of the striker are smaller than the initial impact velocities in value. The part of kinetic energy carried by the striker

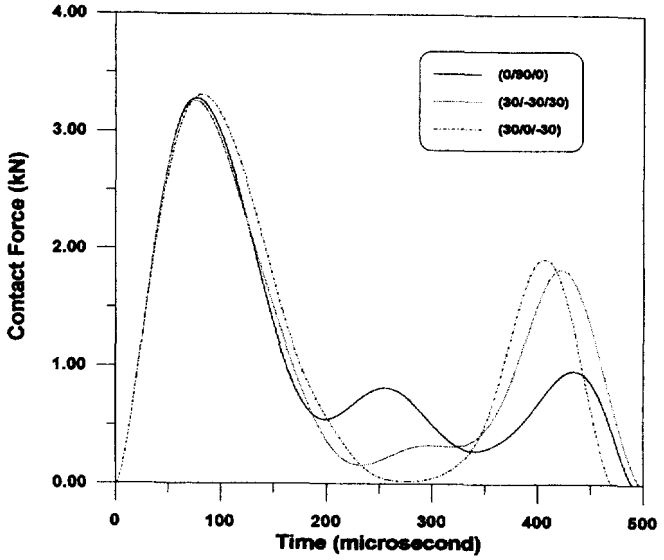

Fig. 6. Histories of contact forces.

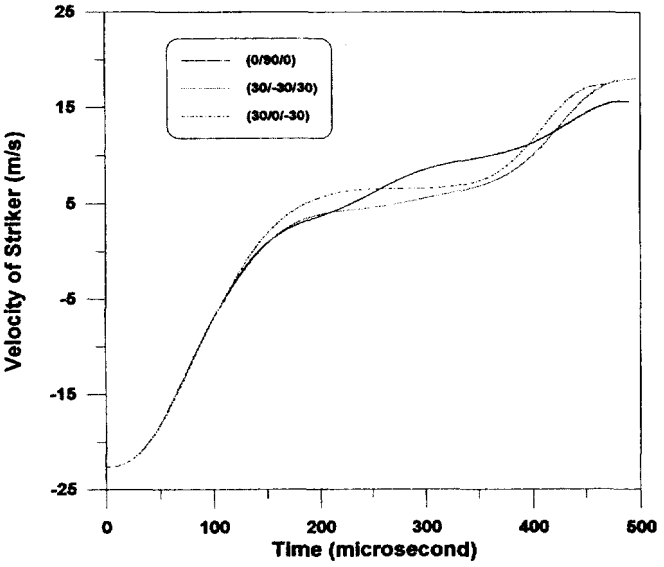

Fig. 7. Variations of the striker's velocity.

is transferred to the laminations. The energies absorbed by the laminated plates, which varied with time, are presented in Fig. 8.

The displacements of the striker and plates at the contact points are plotted as time function in Figs 9–11. The distances between the dash and solid lines represent the local deformation, which is proportional to the contact forces. The displacement of the cross-ply lamination at the contact point is compared with results available in the literature (Sun and Liou, 1989) in Fig. 12. The problem with the same material properties and geometrical configurations was analysed by the finite element method in their work. From the figure, it can be seen that very good agreement is achieved.

The in-plane stresses, σ_x, σ_y and σ_{xy}, at (7, 3.5, 0.1905), which is the mid-point of the line from the impact point to the x-axis and on the upper surface of the laminations, are presented in Figs 13–15. As can be seen, the flexural waves reach the selected point around 10 ms after the impact occurs. In the case of the cross-ply lamination, the σ_{xy} is near to zero, the σ_x and σ_y may be considered as the normal stresses at the point. The transverse shear stresses σ_{yz} and σ_{xz} are checked at the point (7, 3.5 0), which locates on the mid-plane of the plates. The time histories are plotted in Figs 16–17. The transverse shear stresses

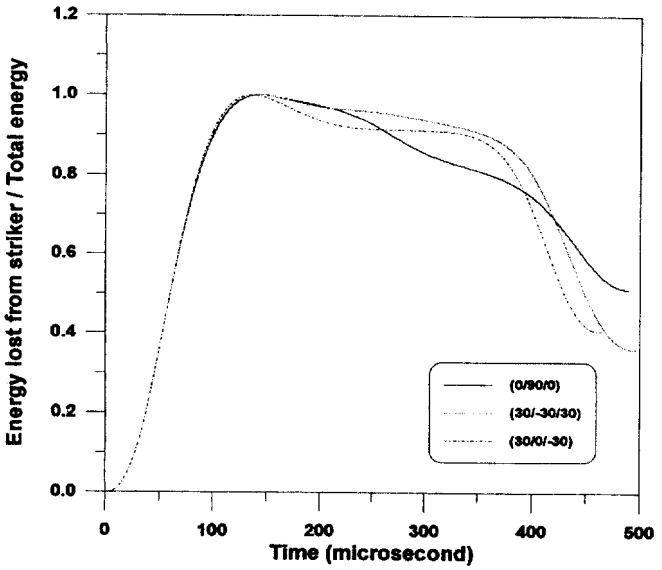

Fig. 8. Energy absorbed by the laminated plates over time.

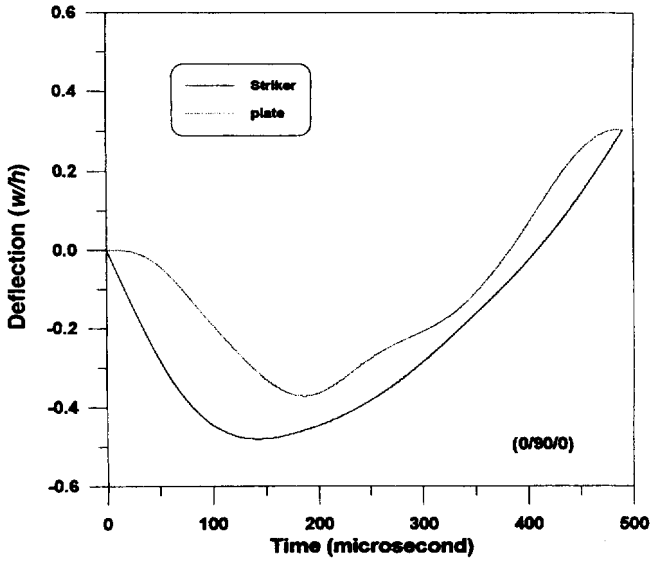

Fig. 9. Displacements of the striker and cross-ply laminated plate at the contact point.

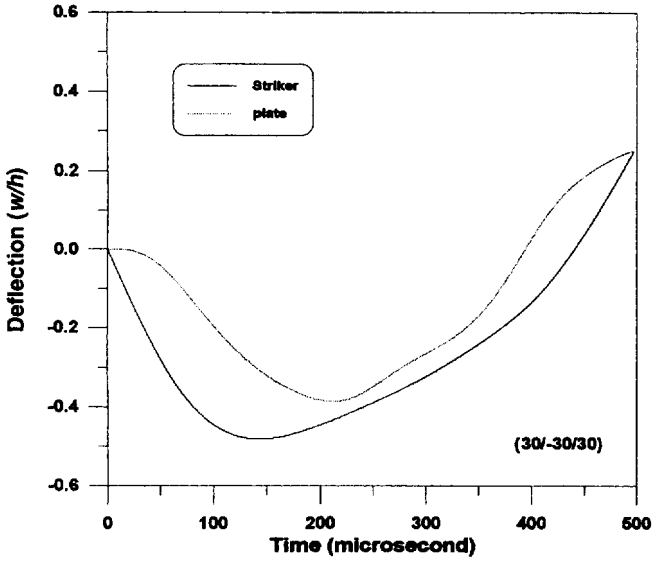

Fig. 10. Displacements of the striker and angle-ply (30/−30/30) laminated plate at the contact point.

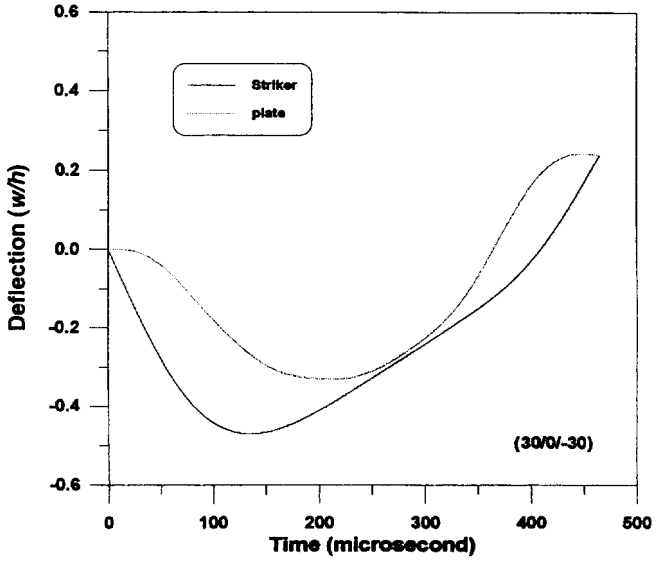

Fig. 11. Displacements of the striker and angle-ply (30/0/−30) laminated plate at the contact point.

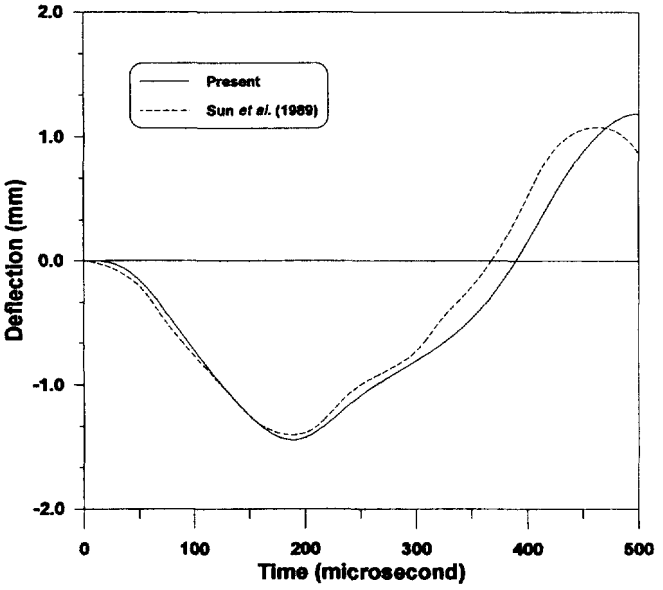

Fig. 12. Comparison of the present result with the existing finite element analysis (Sun and Liou, 1989).

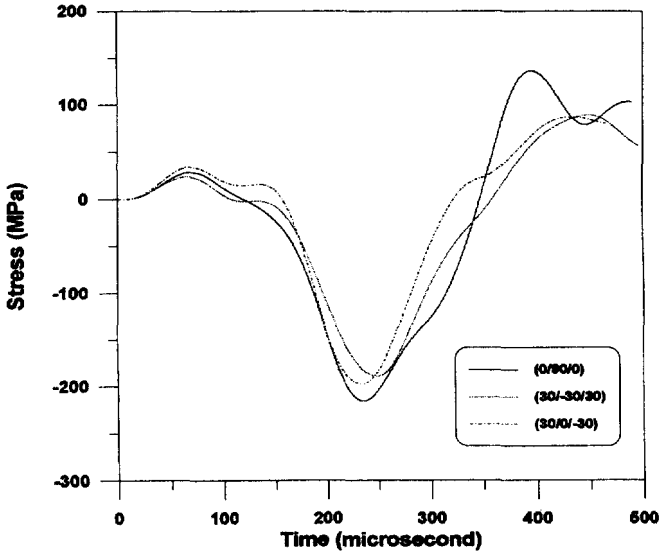

Fig. 13. History of the stress σ_x.

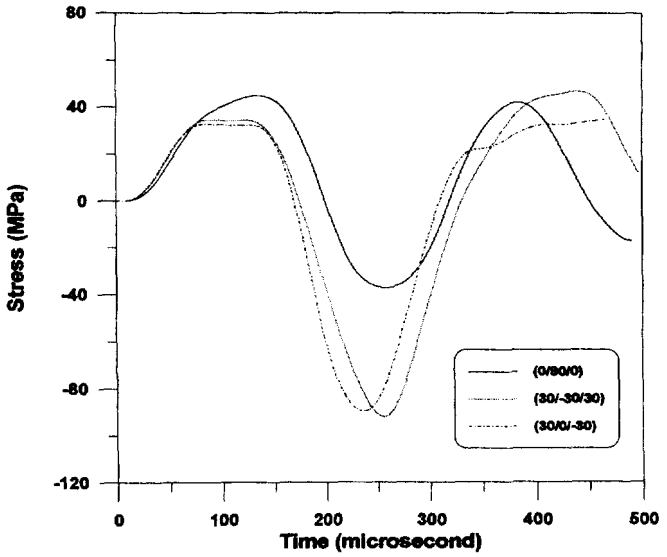

Fig. 14. History of the stress σ_y.

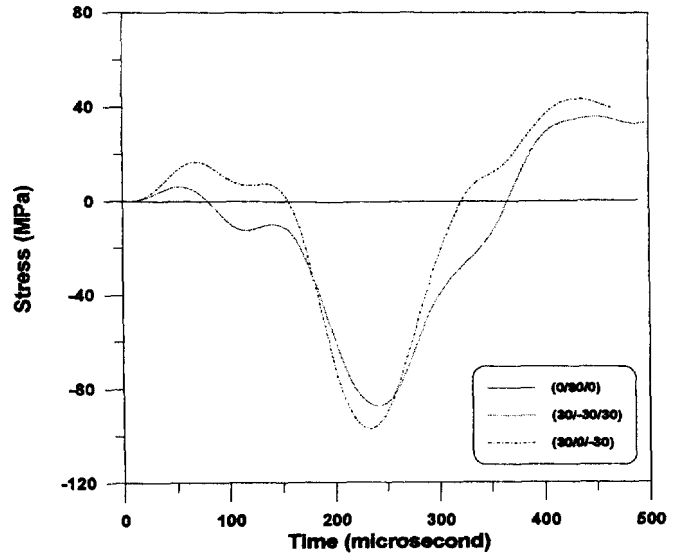

Fig. 15. History of the stress σ_{xy}.

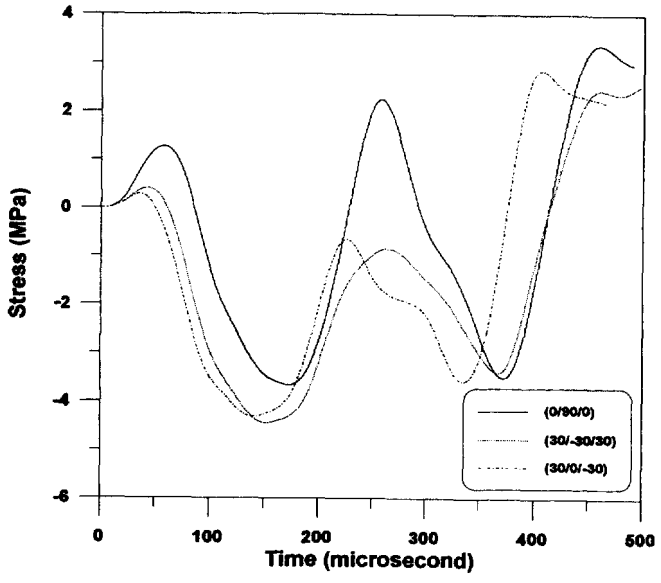

Fig. 16. History of the stress σ_{yz}.

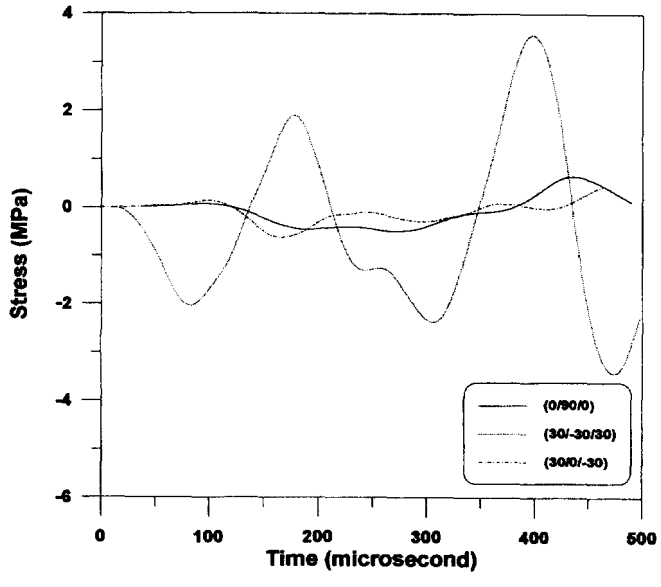

Fig. 17. History of the stress σ_{xz}.

undergo more oscillations during impact and may lead up to delamination inside the composite plates. However, from the scale of the vertical axes, it can be found that the transverse shear stresses are significantly smaller than the in-plane stresses σ_x, σ_y and σ_{xy}. The similar results on the transverse stresses were also found in the finite element analysis (Wu and Chang, 1989).

CONCLUSION

A numerical method is developed to investigate the transient dynamic response of low-velocity impact on laminated composite plates. The non-linear governing equations are derived based on the higher-order shear theory and Hertzian contact law. The method can be used to analyse impact problems of laminated plates with any stacking sequence and boundary conditions. The applicability of the proposed method is verified by comparing the present numerical solutions with those in the published literature.

A low-velocity impact on the cross and angle ply laminated plates with four fixed edges is considered. The effects of the stacking sequences on the dynamic response of composite plates are discussed. The phenomena of the contact force with multiple peak values is observed in all the three types of laminations. The stress histories at any selected point of the plates can be used to predict the delamination damages by employing a suitable stress-based failure criterion.

REFERENCES

Bogdanovich, A. E. and Iarve, E. V. (1992) Numerical analysis of impact deformation and failure in composite plates. *Journal of Composite Materials* **26**(4), 520–545.

Dobyns, A. L. (1981) Analysis of simply-supported orthotropic plates subject to static and dynamic loads. *AIAA Journal* **19**(5), 642–650.

Greszczuk, L. B. (1982) Damage in composite materials due to low velocity impact. In *Impact Dynamics*, ed. Zukas *et al.*, John Wiley & Sons, New York, pp. 55–94.

Hertz, H. (1881) Uber die Beruhrung fester Elasticher Korper. *Journal fur Mathematik* **92**, 156–171.

Karas, K. (1939) Platten unter seitlichem Stoss. *Ingenieur Archiv* **10**, 237–250.

Keer, L. M. and Schonberg, W. P. (1986) Smooth indentation of an isotropic cantilever beam. *International Journal of Solids and Structures* **22**, 87–103.

Lee, E. H. (1940) The impact of a mass striking a beam. *ASME Journal of Applied Mechanics* **62**, 129–138.

Lee, J. D., Du. S. and Liebowitz, H. (1984) Three-dimensional finite element and dynamic analysis of composite laminate subjected to impact. *Computers and Structures* **19**, 807–813.

Lee, Y., Hamilton, J. F. and Sullivan, J. W. (1983) The lumped parameter method for elastic impact problems. *ASME Journal of Applied Mechanics* **50**, 823–827.

Lin, H. J. and Lee, Y. J. (1990) Use of statical indentation laws in the impact analysis of composite laminated plates and shells. *ASME Journal of Applied Mechanics* **57**, 787–789.

NAG (1991) NAG FORTRAN Library Manual. Mark 15, Volume 2.

Ramkumar, R. L. and Chen, P. C. (1983) Low-velocity impact response of laminated plates. *AIAA Journal* **21**(10), 1448–1452.

Reddy, J. N. (1984) A simple higher-order theory for laminated composite plates. *ASME Journal of Applied Mechanics* **51**, 745–752.

Schonberg, W. P., Keer, L. M. and Woo, T. K. (1987) Low velocity impact of transversely isotropic beams and plates. *International Journal of Solids and Structures* **23**(7), 871–896.

Shivakumar, K. N., Elber, W. and Illg, W. (1985) Prediction of impact force and duration due to low-velocity impact on circular composite laminates. *ASME Journal of Applied Mechanics* **52**, 674–680.

Sun, C. T. and Chattopadhyay, S. (1975) Dynamic response of anisotropic laminated plates under initial stress to impact of a mass. *ASME Journal of Applied Mechanics* **42**, 693–698.

Sun, C. T. and Chen, J. K. (1985) On the impact of initially stressed composite laminates. *Journal of Composite Materials* **19**, 490–504.

Sun, C. T. and Liou, W. J. (1989) Investigation of laminated composite plates under impact dynamic loading using a three-dimensional hybrid stress finite element method. *Computers and Structures* **33**(3), 879–884.

Tan, T. M. and Sun, C. T. (1985) Use of statical indentation laws in the impact analysis of laminated composite plates. *ASME Journal of Applied Mechanics* **52**, 6–12.

Timoshenko, S. P. (1913) Zur Frage nach der Wirkung eines Stosse auf einer Balken. *Z. Mathematical Physics* **62**, 198–209.

Whitney, J. M. and Pagano, N. J. (1970) Shear deformation in heterogeneous anisotropic plates. *ASME Journal of Applied Mechanics* **37**, 1031–1036.

Wu, Hsi-Yung T. and Chang, Fu-Kuo (1989) Transient dynamic analysis of laminated composite plates subjected to transverse impact. *Computers and Structures* **31**(3), 453–466.

Yang, S. H. and Sun, C. T. (1982) Indentation law for composite laminates. In *Composite Materials: Testing and Design*, ASTM STP 787, ed. I. M. Daniel, pp. 425–449.

APPENDIX

The mid-plane slopes and transverse displacement can be written as:

$$\Psi_x = \sum_{i=1}^{n} \varphi_{xi}(x, y) A_i(t)$$

$$\Psi_y = \sum_{i=1}^{n} \varphi_{yi}(x, y) B_i(t)$$

$$w = \sum_{i=1}^{n} \varphi_{zi}(x, y) C_i(t). \tag{A.1}$$

The stiffness matrix can then be given by:

$$[K] = \int_0^a \int_0^b \begin{bmatrix} K_{11} & K_{12} & K_{13} \\ K_{21} & K_{22} & K_{23} \\ K_{31} & K_{32} & K_{33} \end{bmatrix} \mathrm{d}x \cdot \mathrm{d}y \tag{A.2}$$

where

$$K_{mn} = K_{nm}^T; \quad K_{mn} = [k_{ij}^{mn}] \quad (m, n = 1, 2, 3)$$

and

$$\begin{aligned}
k_{ij}^{11} &= (A_{55} + 16F_{55}/h^4 - 8D_{55}/h^2)\varphi_{xi}\varphi_{xj} + (D_{11} - 8F_{11}/3h^2 + 16H_{11}/9h^4)\varphi_{xi,1}\varphi_{xj,1} \\
&\quad + (D_{13} - 8F_{13}/3h^2 + 16H_{13}/9h^4)\varphi_{xi,1}\varphi_{xj,2} + (D_{13} - 8F_{13}/3h^2 + 16H_{13}/9h^4)\varphi_{xi,2}\varphi_{xj,1} \\
&\quad + (D_{33} - 8F_{33}/3h^2 + 16H_{33}/9h^4)\varphi_{xi,2}\varphi_{xj,2} \\
k_{ij}^{12} &= (A_{45} + 16F_{45}/h^4 - 8D_{45}/h^2)\varphi_{xi}\varphi_{yj} + (D_{13} - 8F_{13}/3h^2 + 16H_{13}/9h^4)\varphi_{xi,1}\varphi_{yj,1} \\
&\quad + (D_{12} - 8F_{12}/3h^2 + 16H_{12}/9h^4)\varphi_{xi,1}\varphi_{yj,2} + (D_{33} - 8F_{33}/3h^2 + 16H_{33}/9h^4)\varphi_{xi,2}\varphi_{yj,1} \\
&\quad + (D_{23} - 8F_{23}/3h^2 + 16H_{23}/9h^4)\varphi_{xi,2}\varphi_{yj,2} \\
k_{ij}^{13} &= (A_{55} + 16F_{55}/h^4 - 8D_{55}/h^2)\varphi_{xi}\varphi_{zj,1} + (A_{45} + 16F_{45}/h^4 - 8D_{45}/h^2)\varphi_{xi}\varphi_{zj,2} \\
&\quad + (-4F_{11}/3h^2 + 16H_{11}/9h^4)\varphi_{xi,1}\varphi_{zj,3} + (-4F_{12}/3h^2 + 16H_{12}/9h^4)\varphi_{xi,1}\varphi_{zj,4} \\
&\quad + (-8F_{13}/3h^2 + 32H_{13}/9h^4)\varphi_{xi,1}\varphi_{zj,5} + (-4F_{13}/3h^2 + 16H_{13}/9h^4)\varphi_{xi,2}\varphi_{zj,3} \\
&\quad + (-4F_{23}/3h^2 + 16H_{23}/9h^4)\varphi_{xi,2}\varphi_{zj,4} + (-8F_{33}/3h^2 + 32H_{33}/9h^4)\varphi_{xi,2}\varphi_{zj,5} \\
k_{ij}^{22} &= (A_{44} + 16F_{44}/h^4 - 8D_{44}/h^2)\varphi_{yi}\varphi_{yj} + (D_{33} - 8F_{33}/3h^2 + 16H_{33}/9h^4)\varphi_{yi,1}\varphi_{yj,1} \\
&\quad + (D_{23} - 8F_{23}/3h^2 + 16H_{23}/9h^4)\varphi_{yi,1}\varphi_{yj,2} + (D_{23} - 8F_{23}/3h^2 + 16H_{23}/9h^4)\varphi_{yi,2}\varphi_{yj,1} \\
&\quad + (D_{22} - 8F_{22}/3h^2 + 16H_{22}/9h^4)\varphi_{yi,2}\varphi_{yj,2} \\
k_{ij}^{23} &= (A_{45} + 16F_{45}/h^4 - 8D_{45}/h^2)\varphi_{yi}\varphi_{zj,1} + (A_{44} + 16F_{44}/h^4 - 8D_{44}/h^2)\varphi_{yi}\varphi_{zj,2} \\
&\quad + (-4F_{13}/3h^2 + 16H_{13}/9h^4)\varphi_{yi,1}\varphi_{zj,3} + (-4F_{23}/3h^2 + 16H_{23}/9h^4)\varphi_{yi,1}\varphi_{zj,4} \\
&\quad + (-8F_{33}/3h^2 + 32H_{33}/9h^4)\varphi_{yi,1}\varphi_{zj,5} + (-4F_{12}/3h^2 + 16H_{12}/9h^4)\varphi_{yi,2}\varphi_{zj,3} \\
&\quad + (-4F_{22}/3h^2 + 16H_{22}/9h^4)\varphi_{yi,2}\varphi_{zj,4} + (-8F_{23}/3h^2 + 32H_{23}/9h^4)\varphi_{yi,2}\varphi_{zj,5} \\
k_{ij}^{33} &= (A_{55} + 16F_{55}/h^4 - 8D_{55}/h^2)\varphi_{zi,1}\varphi_{zj,1} + (A_{45} + 16F_{45}/h^4 - 8D_{45}/h^2)\varphi_{zi,1}\varphi_{zj,2} \\
&\quad + (A_{45} + 16F_{45}/h^4 - 8D_{45}/h^2)\varphi_{zi,2}\varphi_{zj,1} + (A_{44} + 16F_{44}/h^4 - 8D_{44}/h^2)\varphi_{zi,2}\varphi_{zj,2} \\
&\quad + (16H_{11}\varphi_{zi,3}\varphi_{zj,3} + 16H_{12}\varphi_{zi,3}\varphi_{zj,4} + 32H_{13}\varphi_{zi,3}\varphi_{zj,5} + 16H_{12}\varphi_{zi,4}\varphi_{zj,3} + 16H_{22}\varphi_{zi,4}\varphi_{zj,4} \\
&\quad + 32H_{23}\varphi_{zi,4}\varphi_{zj,5} + 32H_{13}\varphi_{zi,5}\varphi_{zj,3} + 32H_{23}\varphi_{zi,5}\varphi_{zj,4} + 64H_{33}\varphi_{zi,5}\varphi_{zj,5})/9h^4.
\end{aligned}$$

The mass matrix is written as:

$$[M] = \int_0^a \int_0^b \begin{bmatrix} M_{11} & M_{12} & M_{13} \\ M_{21} & M_{22} & M_{23} \\ M_{31} & M_{32} & M_{33} \end{bmatrix} \cdot \mathrm{d}x \cdot \mathrm{d}y \tag{A.3}$$

where

$$M_{mn} = M_{nm}^T; \quad M_{mn} = [m_{ij}^{mn}] \quad (m, n = 1, 2, 3)$$

and

$$\begin{aligned}
m_{ij}^{11} &= (I_2 - 8I_4/3h^2 + 16I_6/9h^4)\varphi_{xi}\varphi_{xj} \\
m_{ij}^{12} &= 0 \\
m_{ij}^{13} &= (-4I_4/3h^2 + 16I_6/9h^4)\varphi_{xi}\varphi_{zj,1} \\
m_{ij}^{22} &= (I_2 - 8I_4/3h^2 + 16I_6/9h^4)\varphi_{yi}\varphi_{yj}
\end{aligned}$$

$$m_{ij}^{23} = (-4I_4/3h^2 + 16I_6/9h^4)\varphi_{yi}\varphi_{zj,2}$$

$$m_{ij}^{33} = I\varphi_{zi}\varphi_{zj} + 16I_6(\varphi_{zi,1}\varphi_{zj,1} + \varphi_{zi,2}\varphi_{zj,2})/9h^4.$$

The coefficients in the matrixes $[K]$ and $[M]$ are defended as follows:

$$(A_{ij}, B_{ij}, D_{ij}, E_{ij}, F_{ij}, H_{ij}) = \sum_{k=1}^{K} \int_{h_{k-1}}^{h_k} Q_{ij}^k(1, z, z^2, z^3, z^4, z^6) \cdot \mathrm{d}z \quad (i,j = 1,2,6)$$

$$(A_{ij}, D_{ij}, F_{ij}) = \sum_{k=1}^{K} \int_{h_{k-1}}^{h_k} Q_{ij}^k(1, z^2, z^4) \cdot \mathrm{d}z \quad (i,j = 4,5)$$

$$(I, I_2, I_4, I_6) = \sum_{k=1}^{K} \int_{h_{k-1}}^{h_k} \rho_k \cdot (1, z^2, z^4, z^6) \cdot \mathrm{d}z. \tag{A.4}$$

The third subscript in admissible functions is defined by:

$$()_{,1} = \frac{\partial()}{\partial x}; \quad ()_{,2} = \frac{\partial()}{\partial y}; \quad ()_{,3} = \frac{\partial^2()}{\partial x^2}; \quad ()_{,4} = \frac{\partial^2()}{\partial y^2}; \quad ()_{,5} = \frac{\partial^2()}{\partial x\,\partial y}. \tag{A.5}$$